J Periodont Res 2006; 41; 259–265

JOURNAL OF PERIODONTAL RESEARCH
doi:10.1111/j.1600-0765.2006.00866.x

An immunohistochemical study of the attachment mechanisms in different kinds of adhesive interfaces in teeth and alveolar bone of the rat

A. K. S. Arambawatta, T. Yamamoto, M. Wakita
Department of Oral Health Science, Hokkaido University, Graduate School of Dental Medicine, Sapporo, Japan

Arambawatta AKS, Yamamoto T, Wakita M. An immunohistochemical study of the attachment mechanisms in different kinds of adhesive intrerfaces in teeth and alveolar bone of the rat. J Periodont Res 2006; 41: 259–265. © Blackwell Munksgaard 2006

Background and Objective: This study was designed to examine the histological and immunohistochemical nature of different kinds of adhesive interfaces in the rat molar region under identical experimental conditions and to discuss the structural and functional similarities between these adhesive interfaces.

Material and Methods: Four kinds of adhesive interfaces – an initial attachment layer for principal fibers on the developing alveolar bone surface, a reattachment layer for principal fibers on resorbed alveolar bone surface, cement lines on the alveolar bone surface unrelated to the principal fibers, and the cemento–dentinal junction – were examined in 25-d-old male Wistar rats. Routine histological staining, immunohistochemical staining for bone sialoprotein and osteopontin, and digestion tests with trypsin were conducted.

Results: The adhesive interfaces showed very similar histological and immunohistochemical features: they were intensely hematoxylin-stainable, deficient in collagen fibrils, and rich in bone sialoprotein and osteopontin. After trypsin treatment the four adhesive interfaces had lost immunoreactivity to bone sialoprotein and osteopontin, and the two adjacent tissue parts held together finally separated at the adhesive interfaces.

Conclusion: The above findings suggest that (i) the different types of adhesive interfaces in the rat molar region have a common structure in that they are filled with highly accumulated bone sialoprotein and osteopontin and deficient in collagen fibrils; (ii) accumulated bone sialoprotein and osteopontin are closely associated with the adhesion at the interfaces; and (iii) the adhesive interfaces have a similar developmental process.

A. K. S. Arambawatta, Department of Oral Health Science, Hokkaido University, Graduate School of Dental Medicine, Kita 13, Nishi 7, Kita-Ku, Sapporo 060–8586, Japan
Tel: +81 11 7064224
Fax: +81 11 7064225
e-mail: kapila@den.hokudai.ac.jp

Key words: bone sialoprotein; cement lines; osteopontin; rat (Wistar male)

Accepted for publication November 9, 2005

When bone resorption and remodeling occur, the newly deposited bone is often demarcated from the older bone by a secreted matrix layer known as 'cement lines' or 'reversal lines', which are intensely stained with hematoxylin. The cement lines are deficient in collagen fibers (1–3) and are rich in noncollagenous bone-related glycoproteins (GPs), osteopontin, and bone sialoprotein (4–7). These GPs are phosphorylated, acid glycoproteins with cell-binding

sequences of an Arg–Gly–Asp (RGD) motif (6,7), and have been suggested to play important roles in the mineralization, matrix–matrix and cell–cell/matrix attachment, and in cell differentiation in mineralized tissue (6–11). Based on the apparent accumulation of bone sialoprotein and osteopontin at cement lines, bone sialoprotein and/or osteopontin have been proposed to act as an interfacial adhesion promoter between 'new' and 'old' mineralized bone, and through this to maintain the overall integrity of mineralized tissue (4–7).

Several types of adhesive interfaces form in the rat molar region. During physiological drifting of rat molars, active osteoclastic resorption and transitory reattachment of principal fibers occur constantly on the alveolar bone surface facing the distal side of teeth (12–17), resulting in one type of cement line. This type of cement line forms on the resorbed bone surface prior to the reattachment of principal fibers, and is stained with hematoxylin, reacts positively for toluidine blue and Alcian blue, but does not stain with silver impregnation. This type of cement line maintains its histological features after it is covered with the Sharpey's fiber containing new bone (= bundles bone) (13–15,17). A different type of cement line forms on resorbed bone surfaces in an area unrelated to the alveolar socket or the principal fibers. This type of cement line also maintains its histological features after it is covered with lamella bone. In addition, unrelated to bone resorption, a specialized layer forms on the alveolar bone surface just prior to the initial attachment of principal fibers (18,19). The histological and immunohistochemical characteristics of this layer are very similar to that of the cement lines. This layer also maintains its histological features after it is covered with bundle bone.

The cemento–dentinal junction has been studied in detail (10,20–31). The cemento–dentinal junction has been found to be very similar to cement lines in histological and immunohistochemical characteristics (17,20,21,31). However, the four types of adhesive interfaces have generally been studied separately under different conditions and there have been no reports comparing all four types of adhesive interfaces in one study under identical experimental conditions.

The purpose of this study was to examine the histological and immunohistochemical characteristics of the four different types of adhesive interfaces under identical experimental conditions, and to elucidate whether these adhesive interfaces are structurally and functionally similar.

Material and methods

Ten 25-d-old Wistar rats, weighing ≈ 50 g, were used. The criterion for the use of this age group in the present study has been delineated in previous studies (18,19,31). All the experimental animals and tissue specimens were treated in accordance with the guidelines for the care and use of laboratory animals of the Experimental Animal Committee, Hokkaido University, Graduate School of Dental Medicine.

General histology

The animals were anesthetized by intraperitoneal injection of sodium pentobarbital, and perfused with 4% (v/v) paraformaldehyde in 0.1 M phosphate buffer (pH 7.4) for ≈ 15 min at room temperature. The maxillae were dissected out, fixed in the same fixative solution for 24 h, and demineralized in 0.2 M ethanolic alkylammonium EDTA (32) for ≈ 2–3 mo at 4°C. After demineralization, the tissues were dehydrated in a graded series of ethanol and embedded in paraffin. Serial sections of 7-μm thickness were cut in the mesiodistal plane of the tooth and either stained with hematoxylin and eosin or silver-impregnated to demonstrate collagen fibers. Some sections were used in digestion tests. They were immersed in 1% (w/v) trypsin (Merck, Darmstadt, Germany) in 0.1 M phosphate buffer (pH 7.0) containing 0.1% (w/v) NaF and 0.4% (w/v) NaCl for ≥ 12 h at 37°C (33). Controls were immersed at 37°C in the same solutions, from which only the enzyme was subtracted. The digested sections and control sections were stained with hematoxylin and eosin.

Immunohistochemistry

Detection of osteopontin and bone sialoprotein Three types of antibodies were used as primary antibodies for the detection of bone sialoprotein [anti-mouse bone sialoprotein rabbit polyclonal antibody (LSL, Tokyo, Japan); anti-human bone sialoprotein rabbit polyclonal antibody (Chemicon, Temecula, Canada); and anti-human bone sialoprotein rabbit polyclonal antibody (Alexis, Lausen, Switzerland)] and osteopontin [anti-mouse osteopontin rabbit polyclonal antibody (LSL); anti-human osteopontin mouse monoclonal antibody (American Research Products, Belmont, MA, USA); and anti-mouse osteopontin rabbit polyclonal antibody (American Research Products)].

After blocking the endogenous peroxidase with 0.3% (v/v) hydrogen peroxide in methanol, the deparaffinized sections were incubated with 2.5% (w/v) testicular hyaluronidase (Sigma Chemical Co., St Louis, MO, USA). Then, the sections were treated with primary antibodies, biotinylated anti-rabbit swine or anti-mouse rabbit polyclonal antibody (Dako, Japan, Kyoto, Japan), and streptavidin–biotin–horseradish peroxidase complex. Finally, they were visualized by the 0.03% 3′-3′ diaminobenzidine method. Normal mouse or rabbit serum was substituted for the primary antibodies in negative controls. Some trypsin-treated sections were also immunostained.

Results

Four locations were selected for examining the structure and composition of the different types of adhesive interfaces. The areas examined are illustrated in Fig. 1.

General histology

Initial attachment layer for principal fibers on the developing alveolar bone surface The initial attachment layer is the layer that functioned in the initial attachment of principal fibers (18,19). This layer was seen in the developing maxillary alveolar bone surface facing the distal root of the second molar

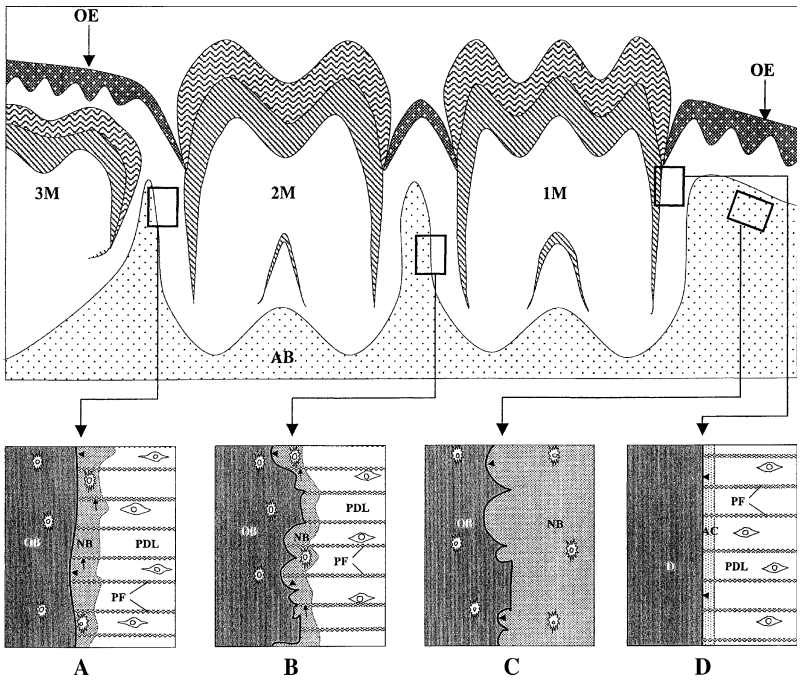

Fig. 1. Diagrammatic illustration of a longitudinally sectioned maxilla in a 25-d-old rat (AB, alveolar bone; OE, oral epithelium; 1M, first molar; 2M, second molar; 3M, third molar). Boxed areas indicate the locations of the different kinds of adhesive interfaces. (A) Initial attachment layer (arrowheads) for principal fibers on the developing alveolar bone surface. (B) Reattachment layer (arrowheads) for principal fibers on the resorbed alveolar bone surface. (C) Cement line (arrowheads) of alveolar bone unrelated to the principal fibers. (D) Cemento–dentinal junction (arrowheads). AC, acellular cementum; arrows, Sharpey's fibers; D, dentine; NB, new bone; OB, old bone; PDL, periodontal ligament; PF, principal fibers.

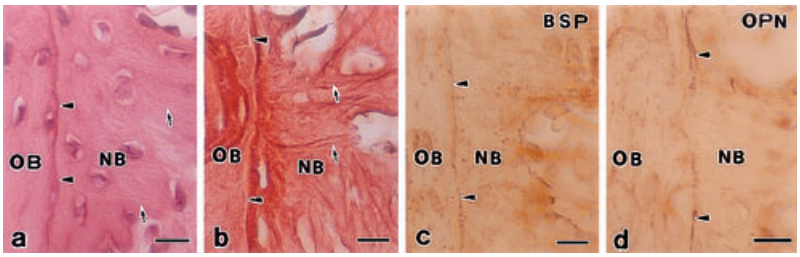

Fig. 2. The initial attachment layer for principal fibers (arrowheads) in sections stained with hematoxylin and eosin (a), silver (b), and anti-bone sialoprotein (c) and anti-osteopontin (d) immunoglobulin. The initial attachment layer is intensely stained with hematoxylin (a) and not impregnated with silver (b). Anti-bone sialoprotein (c) and anti-osteopontin (d) immunoglobulin stain the initial attachment layer most intensely in the bone. Arrows, Sharpey's fibers; NB, new bone; OB, old bone. Bars, 10 μm.

(Fig. 1). The layer was intensely stained with hematoxylin (Fig. 2a) and showed no affinity to silver impregnation (Fig. 2b). Sharpey's fibers of new bone did not cross this layer (Fig. 2-a,b). In sections treated with trypsin for 12 h, the initial attachment layer lost its staining affinity to hematoxylin (Fig. 3a) and appeared as a transparent layer. With further treatment, artificial separation occurred at this layer (Fig. 3b), without showing structural damage to collagen fibers.

Reattachment layer for principal fibers on the resorbed alveolar bone surface The reattachment layer comprises cement line that functioned in the reattachment of principal fibers (15,17). This layer was seen in the alveolar bone surface facing the distal root of the first molar (Fig. 1). This layer was stained with hematoxylin (Fig. 4a), but not impregnated with silver (Fig. 4b). Sharpey's fibers of new bone terminated at this layer, without crossing it (Fig. 4a,b). In the sections digested for 12 h, the layers lost staining affinity to hematoxylin (Fig. 5a), and new bone and old bone were detached with further treatment (Fig. 5b).

Cement lines of alveolar bone unrelated to the principal fibers This type of cement line was seen in the alveolar bone directly covered with the oral epithelium at the site mesial to the first molar. The cement lines were intensely stained with hematoxylin (Fig. 6a). They showed no affinity to silver and appeared as a transparent layer (Fig. 6b). After the digestion test the cement lines lost the staining affinity to hematoxylin (Fig. 7a) and, finally, artificial separation occurred at the cement lines (Fig. 7b).

Cemento–dentinal junction The cemento–dentinal junction of the acellular cementum was examined in the mesial root of the first molars (31). The cemento–dentinal junction appeared as a thin layer, which was more intensely stained with hematoxylin than the rest of the acellular cementum (Fig. 8a). In silver-impregnated sections, the cemento–dentinal junction showed no affinity to silver and appeared as a transparent layer (Fig. 8b). Well-developed principal fibers were arranged at right angles to the cementum surface. The ends of the principal fibers were embedded in the cementum as Sharpey's fibers. In the sections digested for 12 h, the cemento–dentinal junction lost the staining affinity to hematoxylin (Fig. 9a). With further treatment, artificial separation occurred at the junction (Fig. 9b).

Control sections for the digestion test showed the same staining affinity as that in conventionally stained sections (data not shown).

Immunohistochemistry

The three types of anti-bone sialoprotein and anti-osteopontin immunoglobulins provided a similar labeling pattern for bone sialoprotein and osteopontin, respectively. Therefore,

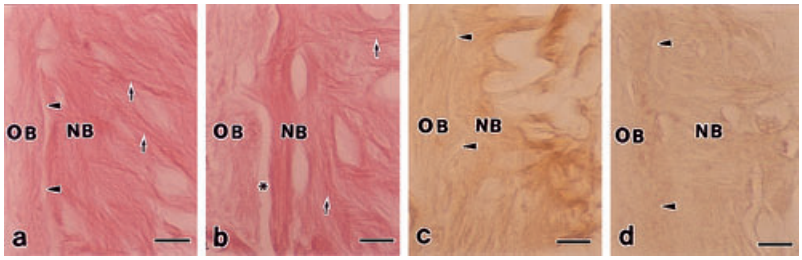

Fig. 3. The initial attachment layer for principal fibers (arrowheads) in sections stained with hematoxylin and eosin (a, b) and with anti-bone sialoprotein (c) and anti-osteopontin (d) immunoglobulin in trypsin-treated sections (a, c, d: 12 h of treatment; b: > 12 h of treatment). After 12 h of treatment, the initial attachment layer has lost staining affinity to hematoxylin (a), and to anti-bone sialoprotein (c) and anti-osteopontin (d) immunoglobulin, and appears as an almost transparent layer. With longer treatment time, the new bone is separated from the old bone at the initial attachment layer (asterisk in b). Arrows, Sharpey's fibers; NB, new bone; OB, old bone. Bars, 10 μm.

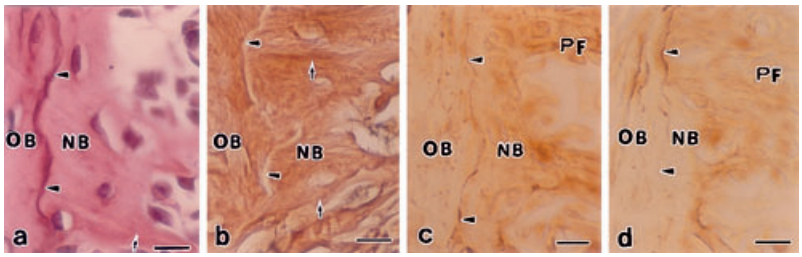

Fig. 4. The reattachment layer for principal fibers (arrowheads) in sections stained with hematoxylin and eosin (a), silver (b), and anti-bone sialoprotein (c) and anti-osteopontin (d) immunoglobulin. The reattachment layer is stained with hematoxylin (a) and not impregnated with silver (b). Anti-bone sialoprotein (c) and anti-osteopontin (d) antibodies stain the reattachment layer most intensely in the bone. Arrows, Sharpey's fibers; NB, new bone; OB, old bone. Bar, 10 μm.

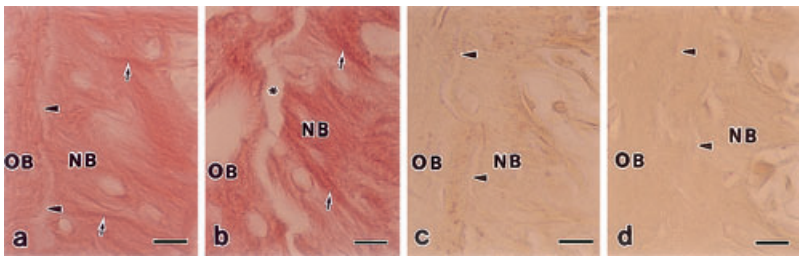

Fig. 5. The reattachment layer (arrowheads) in sections stained with hematoxylin and eosin (a, b) and with anti-bone sialoprotein (c) and anti-osteopontin (d) immunoglobulin in trypsin-treated sections (a, c, d: 12 h of treatment; b: > 12 h of treatment). After 12 h of treatment, the reattachment layer has lost the staining affinity to hematoxylin (a), and to anti-bone sialoprotein (c) and anti-osteopontin (d) immunoglobulin, and appears as an almost transparent layer. With longer treatment time, the new bone is separated from the old bone at the reattachment layer (asterisk in b). Arrows, Sharpey's fibers; NB, new bone; OB, old bone. Bars, 10 μm.

sections stained with antibodies purchased from LSL are shown in the figures. The authenticity of these antibodies to rats has been established in previous studies (19,31,34).

The initial attachment layer for principal fibers on the developing alveolar bone surface, the reattachment layer for principal fibers on the resorbed alveolar bone surface, and the cement lines of alveolar bone unrelated to the principal fibers, showed identical immunohistochemical findings, that is, they showed intense immunoreactivity to both bone sialoprotein (Figs 2c, 4c and 6c) and osteopontin (Figs 2d, 4d and 6d). The bulk of the bone was weakly immunoreactive. After the digestion test, the interfaces lost their immunoreactivity to bone sialoprotein (Figs 3c, 5c and 7c) and osteopontin (Figs 3d, 5d and 7d), and became transparent.

Anti-bone sialoprotein immunoglobulin stained the cementum and the cemento–dentinal junction moderately to intensely, and stained the principal fibers moderately (Fig. 8c). Anti-osteopontin immunoglobulin stained the cemento–dentinal junction and the principal fibers moderately to intensely, but did not stain the rest of the cementum (Fig. 8d). Control sections showed no immunoreaction (data not shown). After 12 h of digestion, the cemento–dentinal junction lost its staining affinity to both bone sialoprotein (Fig. 9c) and osteopontin (Fig. 9d) and became almost transparent.

Discussion

Based on the consistent accumulation of the noncollagenous bone-related GPs, bone sialoprotein, and/or osteopontin in mineralized tissue interfaces in bone and teeth, it has been suggested that these molecules act as an adhesive factor between new and old bone at cement lines (4–7), and at the initial attachment layer for principal fibers on the developing alveolar bone surface (19), as well as between cementum and dentine at the cemento–dentinal junction (31). These adhesive interfaces have been studied separately by different investigators under different conditions, and the data presented in the previous studies were not sufficient to derive conclusions concerning the adhesive function of the two GPs. This study is the first to examine the four different kinds of adhesive interfaces by histological and immunohistological staining under identical conditions in one study and confirms that these adhesive interfaces have common structural features; that is, they are intensely hematoxylin-stainable, deficient in collagen fibrils, and are rich in bone sialoprotein and osteopontin. Furthermore, this study supports the suggestion that the densely

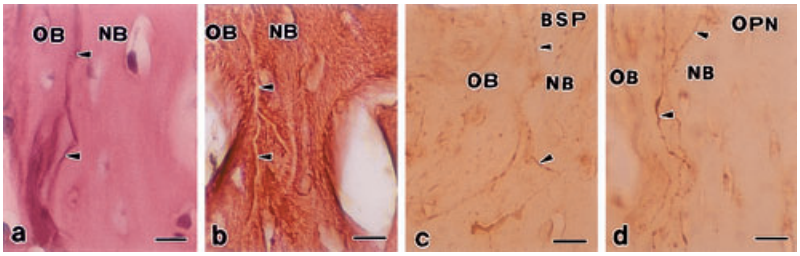

Fig. 6. Cement lines (arrowheads) of alveolar bone unrelated to the principal fibers in sections stained with hematoxylin and eosin (a), silver (b), and anti-bone sialoprotein (c) and anti-osteopontin (d) immunoglobulin. The cement lines are stained with hematoxylin (a) and not impregnated with silver (b). The cement lines are most intensely stained with anti-bone sialoprotein (c) and anti-osteopontin immunoglobulin (d) in the bone. NB, new bone; OB, old bone. Bars, 10 μm.

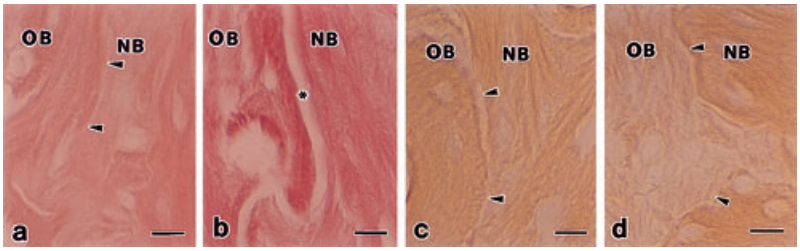

Fig. 7. Cement lines (arrowheads) of alveolar bone unrelated to the principal fibers in sections stained with hematoxylin and eosin (a, b), and with anti-bone sialoprotein (c) and anti-osteopontin (d) immunoglobulin in trypsin-treated sections (a, c, d: 12 h of treatment; b, > 12 h of treatment). After 12 h of treatment, the cement lines have lost the staining affinity to hematoxylin (a), and to anti-bone sialoprotein (c) and anti-osteopontin (d) immunoglobulin, and appear as an almost transparent layer. With longer treatment time the new bone is separated from the old bone at the cement line (asterisk in b). NB, new bone; OB, old bone. Bars, 10 μm.

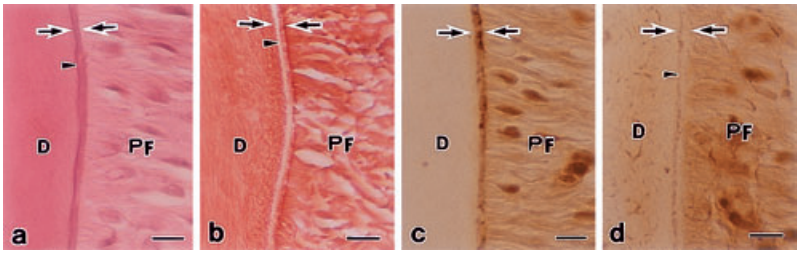

Fig. 8. The cemento–dentinal junction (arrowhead) between the acellular cementum (between arrows) and dentine in sections stained with hematoxylin and eosin (a), silver (b), and anti-bone sialoprotein (c) and anti-osteopontin (d) immunoglobulin. Principal fibers are attached on the cementum surface. The cemento–dentinal junction is intensely stained with hematoxylin (a) and not impregnated with silver (b). The anti-bone sialoprotein immunoglobulin stains the acellular cementum moderately to intensely and the principal fibers moderately (c). The anti-osteopontin stains the cemento–dentinal junction intensely and the principal fibers moderately, but does not stain the rest of the cementum. D, dentine; PF, principal fibers. Bars, 10 μm.

accumulated bone sialoprotein and osteopontin, and not the fibril intermingling, are closely associated with the adhesion at the interfaces in collagen-based hard tissues (19,31).

The adhesive function of bone sialoprotein and osteopontin at these adhesive interfaces was examined by digestion tests. After trypsin treatment, all four types of adhesive interfaces lost immunoreactivity to bone sialoprotein and osteopontin, and were finally broken without structural alterations of collagen fibers. Trypsin digests and depletes most protein polysaccharides (35), but does not degrade collagen fibrils. This has been confirmed by biochemical studies (36–39). Moreover, scanning electron microscopy has revealed that trypsin-treated collagen fibrils maintain the intact fibril structure and orientation without distortion (40). On the basis of these findings and additional findings in the present study, it can be concluded that bone sialoprotein and osteopontin are common adhesive compounds at the different types of interfaces, and the loss of bone sialoprotein and osteopontin causes the artificial detachment.

The above has only considered the GPs, bone sialoprotein and osteopontin as being adhesive factors at the fibril-deficient interfaces. Indeed, the interfaces may contain many noncollagenous matrices other than bone sialoprotein and osteopontin (41), which could be digested with trypsin. In addition, some findings raise questions about the absolute necessity of these noncollagenous GPs in the calcified tissue cohesion (11), as the osteopontin knockout mice develop normally and do not reveal any major bone defects (42). Nevertheless, we would like to propose bone sialoprotein and osteopontin as the main adhesive factors at the interfaces studied here, because (i) bone sialoprotein and osteopontin are the most densely accumulated at the interfaces in the mineralized tissues; (ii) it has been established that bone sialoprotein and osteopontin mediate matrix–matrix adhesion; and (iii) it has not yet been reported that other matrices provide stronger adhesion than bone sialoprotein and osteopontin. However, it is premature to conclude that bone sialoprotein and osteopontin are the only factors maintaining the integrity of these interfaces. When mineral formation and its deposition are inhibited in nonspecific alkaline phosphatase knockout mice, the deposition of the noncollagenous matrix is also prevented and, as a result, the principal fibers are not firmly anchored by Sharpey's fibers (43). Moreover, it is still unknown how the interdigitation of the mineral crystallites is involved in the interface integrity, because this study only examined demineralized sections. To

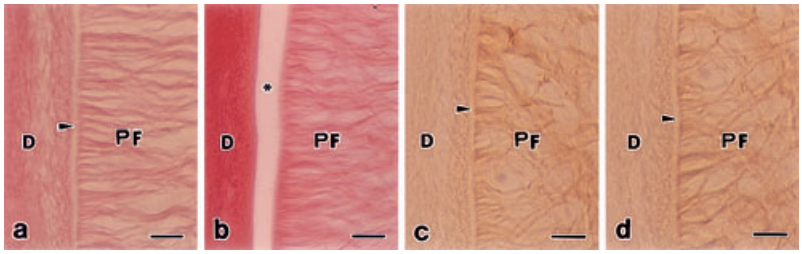

Fig. 9. The cemento–dentinal junction (arrowhead) in sections stained with hematoxylin and eosin (a, b), and with anti-bone sialoprotein (c) and anti-osteopontin (d) immunoglobulin in trypsin-treated sections (a, c, d: 12 h of treatment; b, > 12 h of treatment). After 12 h of treatment, the cemento–dentinal junction has lost the staining affinity to hematoxylin (a) and anti-bone sialoprotein (c) and anti-osteopontin (d) immunoglobulin, and appears as an almost transparent layer. With longer treatment time the acellular cementum is split from the root dentine at the cemento–dentinal junction (asterisk in b). D, dentine; PF, principal fibers. Bars, 10 μm.

date we assume that bone sialoprotein and osteopontin provide the firmness of the interfaces in co-operation with a still-unknown complex system.

The development of one type of adhesive interface, the cemento–dentinal junction, has been studied extensively in human and rat molars by light, transmission, and scanning-electron microscopy (10,20–31). In a series of articles, Yamamoto *et al.* reported that (i) with the initial dentin calcification in rat acellular cementogenesis, a hematoxylin-stained and bone sialoprotein and osteopontin-rich initial cementum layer formed on the calcified dentine surface; (ii) successively the initial or primitive principal fibers attached on this layer; and (iii) after the acellular cementum had been established, the initial cementum layer remained as the cemento–dentinal junction, maintaining the structural features (20,21,28,29,31). From these findings, they suggested that (i) complicated intermingling would not occur between already calcified dentinal fibrils and principal fibers; (ii) therefore, the bone sialoprotein- and osteopontin-rich layer is necessary to mediate the initial principal fibers attachment; and (iii) as a result, the cemento–dentinal junction becomes fibril-poor.

Regarding the cellular cementogenesis, no agreement has been reached on the details of the initial development of the cemento–dentinal junction. Bosshardt *et al.* (10) reported that the overlapping and interlacement of collagen fibrils occurred at the dentino–cemental interface. Yamamoto *et al.* (34) reported that in the cellular cementogenesis, the cemento–dentinal junction developed differently in mesial and distal surfaces in the same root: in the mesial surface, the cemento–dentinal junction containing only a few fibrils forms; in contrast, in the distal surface the cemento–dentinal junction containing the interlacement of dentinal and cemental fibrils forms. An answer to details of the dentine–cellular cementum attachment awaits further investigation.

We have studied the development of the initial attachment layer for principal fibers on the developing alveolar bone surface (18,19). In several aspects, the development of the layer is similar to that of the cemento–dentinal junction in the acellular cementum.

(i) The alveolar bone surface is almost completely mineralized and osteoid is discernible only in places, prior to the appearance of the initial attachment layer.

(ii) The hematoxylin-stainable and bone sialoprotein- and osteopontin-rich initial attachment layer appears on the bone surface, after which the initial principal fibers attach onto the layer.

(iii) After the layer is covered with the new bone, it remains between the new and the old bone, maintaining the intense immunoreactivity to bone sialoprotein and osteopontin.

These findings suggest that the developmental process is similar between the initial attachment layer and the cemento–dentinal junction (in acellular cementum), and that the initial attachment layer develops necessarily to anchor the initial principal fibers. A similar interpretation could be applied to the reattachment layer. The reattachment layer forms on the resorbed alveolar bone surface at the interdental septum and/or interadicular septum prior to the reattachment of principal fibers, and then principal fibers reattach onto the layer (13–15). Similarly, it is common knowledge that hematoxylin-stainable, fibril-poor, and bone sialoprotein- and/or osteopontin-rich cement lines form on the resorbed bone surface prior to the deposition of new bone matrices (3–5,44). On the basis of these data, it is reasonable to consider that the four different adhesive interfaces develop in a similar manner to bind the collagen fibrils of newly formed hard tissue and, after the new hard tissue has formed, the adhesive interfaces function to bind the established tissue.

In conclusion, we suggest that (i) the different types of adhesive interfaces in rat molar region have a common structure; they are filled with highly accumulated noncollagenous bone-related GPs, bone sialoprotein, and osteopontin and are deficient in collagen fibrils. (ii) Accumulated bone sialoprotein and osteopontin are closely associated with adhesion at the adhesive interfaces (iii). The developmental process of the adhesive interfaces is similar.

The origin of the matrices of the four adhesive interfaces is still undetermined. Therefore, further studies will be required to elucidate which cells produce the noncollagenous GPs and the factors that induce the formation of the interfaces.

References

1. Frasca P. Scanning-electron microscopy studies of 'ground substance' in the cement lines, resting lines, hypercalcified rings and reversal lines of human cortical bone. *Acta Anat* 1981;**109:**115–121.
2. Schaffler MB, Burr DB, Frederickson RG. Morphology of the osteonal cement line in human bone. *Anat Rec* 1987;**217:**223–228.
3. Zhou H, Chernecky R, Davies JE. Deposition of cement at reversal lines in rat femoral bone. *J Bone Miner Res* 1994;**9:**367–374.

4. McKee MD, Nanci A. Osteopontin at mineralized tissue interfaces in bone, teeth, and osseointegrated implants: ultrastructural distribution and implications for mineralized tissue formation, turnover, and repair. *Microsc Res Tech* 1996;**33:**141–164.
5. McKee MD, Nanci A. Osteopontin: an interfacial extracellular matrix protein in mineralized tissues. *Connect Tissue Res* 1996;**35:**197–205.
6. Ganss B, Kim RH, Sodek J. Bone sialoprotein. *Crit Rev Oral Biol Med* 1999;**10:**79–98.
7. Sodek J, Ganss B, McKee MD. Osteopontin. *Crit Rev Oral Biol Med* 2000;**11:**279–303.
8. MacNeil RL, Berry J, D'Errico J, Strayhorn C, Piotrowski B, Somerman MJ. Role of two mineral-associated adhesion molecules, osteopontin and bone sialoprotein, during cementogenesis. *Connect Tissue Res* 1995;**33:**1–7 [323–329].
9. McKee MD, Zalzal S, Nanci A. Extracellular matrix in tooth cementum and mantle dentin: localization of osteopontin and other noncollagenous proteins, plasma proteins, and glycoconjugates by electron microscopy. *Anat Rec* 1996;**245:**293–312.
10. Bosshardt DD, Zalzal S, McKee MD, Nanci A. Developmental appearance and distribution of bone sialoprotein and osteopontin in human and rat cementum. *Anat Rec* 1998;**250:**13–33.
11. Nanci A. Content and distribution of noncollagenous matrix proteins in bone and cementum: relationship to speed of formation and collagen packing density. *J Struct Biol* 1999;**126:**256–269.
12. Kraw AG, Enlow DH. Continuous attachment of the periodontal membrane. *Am J Anat* 1967;**120:**133–148.
13. Kurihara S, Enlow DH. An electron microscopic study of attachments between periodontal fibers and bone during alveolar remodeling. *Am J Orthod* 1980;**77:**516–531.
14. Kurihara S, Enlow DH. A histochemical and electron microscopic study of an adhesive type of collagen attachment on resorptive surfaces of alveolar bone. *Am J Orthod* 1980;**77:**532–546.
15. Johnson RB. A classification of Sharpey's fibers within the alveolar bone of the mouse: a high voltage electron microscope study. *Anat Rec* 1987;**217:**339–347.
16. Kuroiwa M, Chihara K, Higashi S. Light and electron microscopic observation of attachment between the periodontal ligament and alveolar bone in rat molars. *Showa University J Med Sci* 1994;**6:** 165–170.
17. Islam MN, Yamamoto T, Wakita M. A light microscopic study of the attachment mechanism in different kinds of adhesive lines in rat molars. *Ann Anat* 2001;**183:**319–323.
18. Islam MN, Yamamoto T, Wakita M. Light and electron microscopic study of the initial attachment of principal fibers to the alveolar bone surface in rat molars. *J Periodont Res* 2000;**35:**344–351.
19. Arambawatta AKS, Yamamoto T, Wakita M. Immunohistochemical characterization of noncollagenous matrix molecules on the alveolar bone surface at the initial principal fiber attachment in rat molars. *Ann Anat* 2005;**187:**77–87.
20. Yamamoto T. The innermost layer of cementum. its ultrastructure, development, and calcification. *Arch Histol Jpn* 1986;**49:**459–481.
21. Yamamoto T, Wakita M. Initial attachment of principal fibers to the root dentin surface in rat molars. *J Periodont Res* 1990;**25:**113–119.
22. Bosshardt DD, Schroeder HE. Initiation of acellular extrinsic fiber cementum on human teeth: a light- and electron microscopic study. *Cell Tissue Res* 1991;**263:**311–324.
23. Bosshardt DD, Schroeder HE. Establishment of acellular extrinsic fiber cementum on human teeth: a light- and electron microscopic study. *Cell Tissue Res* 1991;**263:**325–336.
24. Bosshardt DD, Schroeder HE. Cementogenesis reviewed: a comparison between human premolars and rodent molars. *Anat Rec* 1996;**245:**262–292.
25. Yamamoto T, Domon T, Takahashi S, Islam MN, Suzuki R, Wakita M. The structure and function of the cemento-dentinal junction in human teeth. *J Periodontal Res* 1999;**34:**261–268.
26. Yamamoto T, Domon T, Takahashi S, Islam MN, Suzuki R. The fibrous structure of the cemento-dentinal junction in human molars shown by scanning electron microscopy combined with NaOH-maceration. *J Periodont Res* 2000;**35:**59–64.
27. Yamamoto T, Domon T, Takahashi S, Suzuki R, Islam MN. The fibrillar structure of cement lines on resorbed root surfaces of human teeth. *J Periodont Res* 2000;**35:**208–213.
28. Yamamoto T, Domon T, Takahashi S, Islam MN, Suzuki R, Wakita M. The structure of the cemento-dentinal junction in rat molars. *Ann Anat* 2000;**182:**185–190.
29. Yamamoto T, Domon T, Takahashi S, Islam MN, Suzuki R. The fibrillar structure of cementum and dentin at the cemento-dentinal junction in rat molars. *Ann Anat* 2000;**182:**499–503.
30. Yamamoto T, Domon T, Takahashi S, Islam MN, Suzuki R. The fibrillar structure of the cemento-dentinal junction in different kinds of human teeth. *J Periodont Res* 2001;**36:**317–321.
31. Yamamoto T, Domon T, Takahashi S, Arambawatta AKS, Wakita M. Immunolocalization of proteoglycans and bone-related noncollagenous glycoproteins in developing acellular cementum of rat molars. *Cell Tissue Res* 2004;**317:**299–312.
32. Scott JE, Kyffin TW. Demineralization in organic solvents by alkylammonium salts of ethylenediaminetetra-acetic acid. *Biochem J* 1978;**169:**697–701.
33. Yamada K. Proteins. In: Ogawa K, Takeuchi T, Mori T, eds. *New Histochemistry*. Tokyo: Asakura-shoten, 1975: 439–463. [In Japanese.]
34. Yamamoto T, Domon T, Takahashi S *et al*. Determination of two different types of cellular cementogenesis in rat molars: a histological and immunohistochemical study. *Matrix Biol* 2005;**24:**295–305.
35. Harris ED Jr, Parker HG, Radin EL, Krane SM. Effects of proteolytic enzymes on structural and mechanical properties of cartilage. *Arthritis Rheum* 1972;**15:**497–503.
36. Ochi J. Histochemistry. A carbohydrate. In: Sano Y, ed. *Histological Techniques*. Tokyo: Nanzando, 1985: 452–469. [In Japanese.]
37. Smalley JW, Birss AJ, Shuttleworth CA. The degradation of type I collagen and human plasma fibronectin by the trypsin-like enzyme and extracellular membrane vesicles of *Bacteroides gingivalis* W50. *Arch Oral Biol* 1988;**33:**323–329.
38. Welgus HG, Grant GA. Degradation of collagen substrates by a trypsin-like serine protease from the fiddler crab *Uca pugilator*. *Biochemistry* 1983;**22:**2228–2233.
39. Miller EJ, Finch JE Jr, Chung E, Butler WT, Robertson PB. Specific cleavage of the native type III collagen molecule with trypsin. Similarity of the cleavage products to collagenase-produced fragments and primary structure at the cleavage site. *Arch Biochem Biophys* 1976;**173:**631–637.
40. Segawa K, Takiguchi R. Ultrastructural alteration of cartilaginous fibril arrangement in the rat mandibular condyle as revealed by high-resolution scanning electron microscopy. *Anat Rec* 1992;**234:**493–499.
41. Robey PG. Vertebrate mineralized matrix proteins: structure and function. *Connect Tissue Res* 1996;**35:**131–136.
42. Rittling SR, Matsumoto HN, McKee MD *et al*. Mice lacking osteopontin show normal development and bone structure but display altered osteoclast formation *in vitro*. *J Bone Miner Res* 1998;**13:**1101–1111.
43. Beertsen W, VandenBos T, Everts V. Root development in mice lacking functional tissue non-specific alkaline phosphatase gene: inhibition of acellular cementum formation. *J Dent Res* 1999;**78:**1221–1229.
44. Chen J, McCulloch CA, Sodek J. Bone sialoprotein in developing porcine dental tissues: cellular expression and comparison of tissue localization with osteopontin and osteonectin. *Arch Oral Biol* 1993;**38:**241–249.